5-2016

Improving and Understanding Inter-filament Bonding in 3D-printed Polymers

Madeline S. Stark
University of Tennessee, Knoxville, mstark1@vols.utk.edu

Improving and Understanding Inter-filament Bonding in 3D-printed Polymers

A Thesis Submitted to the Faculty

Of The University of Tennessee

by Madeline S. Stark

May 2016

Department of Chemistry, The University of Tennessee, Knoxville TN

Honors Thesis, The University of Tennessee, Chancellor's Honors Program

Thesis Defense Committee:

Dr. Mark Dadmun, Advisor

Dr. Brett Compton

Dr. Bin Zhao

TABLE OF CONTENTS

List of Tables and Figures

Improving and Understanding Inter-filament Bonding in 3D-printed Polymers

Abstract

This paper examines the inter-filament bonding within Fused Deposition Modeling (FDM) 3D printed parts as well as the covalent modification of acrylonitrile-butadiene-styrene (ABS) copolymer. A fundamental limitation of 3D printed parts is that they are affected by anisotropy, which results in weak inter-filament bonding. Chemical cross-linkers were applied to the interface of T-peel samples to increase the inter-filament bonding of 3D printed parts in the z-direction. The interfacial adhesion between adjacent layers was quantified using the T-peel test and inter-filament bonding was improved with 4,4′-diaminodiphenylmethane (DADPM) as the chemical cross-linker.

Additionally, the post-polymerization modification of ABS was demonstrated through a thiol-ene “click” reaction. The thiol-modified ABS was characterized using ^{1}H-NMR spectroscopy. Percent composition of the modified ABS calculated from peak integrations indicate that the thiol added to the polybutadiene segments. These studies increase our understanding of chemically crosslinking layers in FDM to improve the strength of 3D printed parts and provide pathways to covalent bond formation between adjacent layers within the part. Further improvements to FDM technology will allow for the creation of mechanically robust, geometrically complex parts that are useful in a wide range of applications.

Chapter 1: Introduction

Additive manufacturing (AM), the production of 3D objects, has rapidly become a method of creating prototypes for manufacturing. Unlike traditional manufacturing techniques which utilize molds or welding, AM involves layer-by-layer synthesis of parts. The layer-by-layer process allows for greater freedom of design and flexibility of shape and part orientation in the manufacturing industry. With this rapid growth comes the need to understand the technique as well as improve the methodology. A common AM technique is Fused Deposition Modeling (FDM). In FDM, a 3D model is created in AutoCAD and the STL file is sent to SlicR, a program that slices the model into thin layers. These layers represent the 2D sections that, when stacked on top of each other, emulate the 3D printed object[1]. Once the layers have been generated, the g-code is sent to the 3D-printer. The polymer filament passes through the heating element, which is heated to a temperature just below the melting point of the polymer[1]. Upon passing through the heating element the filament becomes semi-molten, goes through the extrusion nozzle and is then deposited layer-by-layer on a glass bed platform. During the printing process, the printer head moves in the X-Y plane according to the geometry specified by the software while the platform adjusts in the Z-direction so that new layers can be deposited.

Thermoplastic polymers are ideal filaments for FDM applications since they soften above a certain temperature and solidify below that temperature[2]. Above the critical temperature, a thermoplastic can be molded or extruded and then cooled. However, many thermoplastic polymers such as polystyrene are rigid and brittle, which limits their applications in manufacturing, where toughness is critical to creating quality

parts. To increase the toughness of brittle polymers, an elastomer is added to form a copolymer with two phases. Acrylonitrile-butadiene-styrene (ABS) is one such copolymer. In this polymer, dispersed butadiene particles make up the rubbery phase and contribute to toughness, while poly(styrene-*co*-acrylonitrile) (SAN) is responsible for the formability of the polymer[3]. Since the butadiene particles have layers of SAN grafted onto their surfaces, the two phases are capable of interacting, creating a polymer that is both tough and moldable[3]. ABS is a common material for traditional manufacturing techniques, particularly injection molding, due to its toughness and moldability[4]. Currently, it is used in the production of car parts, household appliances, medical devices, and a variety of other applications[2]. Because of its importance in the plastics industry, ABS is one of the target thermoplastics for FDM applications.

The next step in the growth of additive manufacturing is transitioning from prototyping parts to manufacturing them using FDM or similar techniques. However, the leading drawback to replacing traditional manufacturing techniques with FDM is that 3D-printed parts lack the toughness, impact strength and consistency of manufactured parts[5]. This lack of quality is mainly due to anisotropy, the property of being directionally dependent, which affects 3D-printed parts. In FDM, filament is laid down layer-by-layer in a crisscross manner and once the molten filament is extruded, the heat dissipates rapidly. By the time the next layer is deposited, the first layer has cooled and therefore diffusion between the two layers is limited. Perpendicular to the printed layers, the interlayer adhesion is particularly weak, limiting toughness and robustness[6]. Since the 3D-printed part's properties are not identical in all directions, studies have found that anisotropy can reduce the impact strength by as much as 90%[7] and the tensile strength

by as much as 85 %[8]. Thus, reducing anisotropy is one of the foremost challenges in transitioning FDM technology from prototyping to manufacturing parts. Previous studies have attempted to understand and mechanically reduce anisotropy in 3D-printed parts by changing print orientation, or the printing path[6–8]. Other research has chemically modified the copolymer, incorporating carbon nanofibers[9] or glass fiber into the ABS filament[10]. Although these methods have resulted in parts with greater stiffness and strength, printed part flexibility and handleability are significantly reduced.

Chemical crosslinking is another method of improving adhesion between adjacent layers. Crosslinking involves the formation of either noncovalent or covalent bonds between polymer chains. A variety of experiments have investigated the formation of noncovalent bonds in polymer systems, including ionic crosslinks in carboxylated-nitrile rubber (XNBR)[11] and hydrogen bonding in the supramolecular network of maleated polyethylene-octene elastomer[12]. In the aforementioned cases, the noncovalent crosslinking resulted in improved mechanical properties for the tested polymer systems. It is unlikely, however, that noncovalent crosslinking would be amenable to FDM applications since noncovalent interactions are not as resistant to the higher temperatures required by FDM as covalent bonds. For example, covalent crosslinking of epoxy resins utilizing diamines as chemical hardeners has resulted in materials with greater tensile strength but these materials have not been sufficiently studied for FDM applications[13]. Additionally, ionizing gamma radiation has been shown to effectively increase the chemical resistance while reducing anisotropy in 3D-printed shape memory polymers when used as a crosslinking agent[14]. Consistent exposure to penetrating gamma rays, however, poses a health risk to the operator and can cause

cellular damage. Therefore, a more user-friendly crosslinking technique that promotes the formation of covalent bonds is needed.

The question of crosslinking centers on whether or not covalent bonds can form between polymer chains of adjacent layers in FDM. For this to occur, the ABS filament must be amenable to post-polymerization modification. Post-polymerization modification is a powerful tool for creating functional materials since it involves the direct reaction of functional groups that are inert to polymerization conditions but can readily convert into a broad range of other functional groups. This method is convenient for functionalizing polymeric-active esters with amine groups as well as activated alkenes with thiols through a Michael Addition reaction in mild conditions[15]. Although not a novel method of modifying polymers, radical thiol addition has also been investigated recently to functionalize polymeric alkenes, such as 1,2-polybutadiene[16]. In the presence of UV-light or a radical source, thiols add to the least substituted carbon of the double bond (Figure 1).

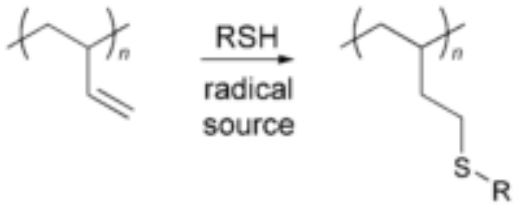

Figure 1: *Thiol radical addition proceeds in an anti-Markovnikov fashion[15].*

Such “click reactions” have several benefits, namely that they have high yields, good specificity and minimal byproducts. Current research has utilized the thiol-ene click

reaction to create cross-linked polymeric matrices for synthetic, degradable hydrogels[17], dental restorative materials[18] as well thermo-sensitive electrospun fibers[19]. Although Campos and Hawker describe the thermal and photochemical thiol-ene click reactions for a diverse array of polymer systems[20], to date, ABS has not been characterized using these methods. Since the butadiene component of ABS contains a double bond capable of reacting with the thiol under a UV or radical source, it is a potential substrate for the thiol-ene click reaction. Consequently, demonstrating that post-polymerization modification is a viable option for ABS would provide a pathway to form covalent bonds between the adjacent layers of ABS filament during the print process.

Therefore, this experimental research program seeks to address the efficacy of chemical cross-linking to improve the quality of inter-filament bonding as well as to demonstrate the post-polymerization modification of ABS to create filament that can readily undergo post-deposition cross-linking reactions between layers.

Chapter 2: Materials and Methods

2.1 Interfacial adhesion measurements

To determine the interfacial adhesion between layers of the 3D printed parts, six T-peel samples were printed for each sample set (Figure 2).

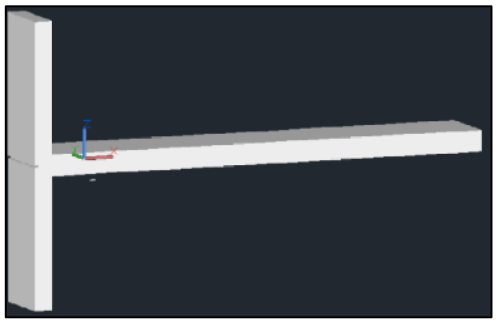

Figure 2: *Model of a representative T-peel sample.*

For the first three sample sets, the bottom portions of the samples were printed and the printing was then paused for either 0, 30 or 60 minutes. The purpose of the pause times was to determine the effect of cooling of the layer on the strength of adhesion between the layers. Before restarting the printer, the surface temperature of the printed part was recorded with an IR-thermometer to quantify the amount of heat lost during the pause time. The t-peel test was utilized to determine the strength of the interface.

For the second set of samples, the printer was once again paused for 0, 30 and 60 minutes. After each pause time, however, a layer of a chemical cross-linker was painted onto the exposed surface of the bottom portion of the part before resuming printing. The chemical cross-linkers utilized were 2,2-azobisisobutanitrile (AIBN), copper (II) sulfate pentahydrate and 4,4′-diaminodiphenylmethane (DADPM). The cross-linkers were selected to react with the functional groups of ABS. In $CuSO_4$, the Cu^{2+} ions can form coordination bonds with the acrylonitrile groups on contiguous layers. Alternatively, AIBN decomposes into radicals that can react with the C-C double bond of butadiene

and initiate the formation of covalent bonds between adjacent layers. DADPM should also react with the carboxyl groups resulting from the degradation of butadiene during deposition. All three solutions were 10 % by weight in acetone. To prepare the copper (II) sulfate solution, the blue copper sulfate hydrate was first heated to remove water and form $CuSO_4$ and was then suspended in acetone to create a 10 % by weight solution. It is hoped that the addition of a chemical cross-linker will chemically bond adjacent layers together and improve the strength of the interlayer adhesion. To quantify the effect of adding the cross-linkers, the interfacial adhesion of the interface was measured using the T-peel test.

The T-peel test was applied to the samples to determine the interfacial adhesion between the two layers. The DADPM and $CuSO_4$ experiments were performed on a custom Universal Testing Machine (UTM) at Oak Ridge National Laboratory (Figure 3). The load cell was 50 lbs. and the rate of testing was 0.069 in/min. The AIBN experiments were performed on the Instron at the University of Tennessee's Center for Renewable Carbon, at a rate of 2.1×10^{-3} mm/s with a 100 lbs. load cell (Figure 4).

Figure 3: *T-peel test on ORNL's UTM*

Figure 4: *Instron testing machine*

Once the force required to peel the samples was obtained, the interfacial adhesion (G_a) was calculated using the equation: $G_a = \frac{F}{W}$, where F is the force needed to separate the layers in Newtons and W is the width of the sample in meters.

2.2 Thermal thiol-ene polymerization modification

To determine whether covalent bonds can form after polymerization, a series of thiol-ene polymerization reactions using a procedure similar to that described by Campos and Hawker were performed[20]. In these experiments, ABS polymer beads, 5-10 equivalents (with respect to the alkene) of thiol, and 0.50 equivalent of AIBN were added to an ampule. The thiols utilized in the experiments were 2,2-(ethylenedioxy)diethanethiol (DODT) and cysteamine (Figure 5).

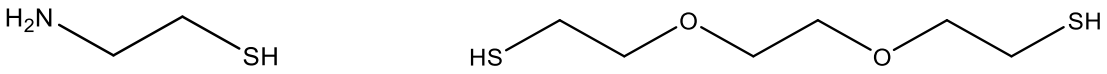

Figure 5: *Shows the structures of cysteamine (L) and 2,2'-(ethylenedioxy)diethanethiol (R).*

A minimal amount of THF was added to solubilize all components. Next, the solution mixtures were degassed using three freeze-pump-thaw cycles, and then heated at 80 ^{o}C for 2 hours. Once the reaction was complete, the modified polymers were purified by precipitation into ethanol. The purified polymers were then characterized using ^{1}H-NMR spectroscopy at 300 MHz in $CDCl_3$.

Chapter 3: Results and Discussion

Interfacial adhesion measurements

Figures 6 and 7 show the interfacial adhesion measurements using data from the t-peel tests. The black squares on both figures represent the neat ABS, where no chemical cross-linkers were applied. Samples treated with a $CuSO_4$ solution are represented by the blue triangles on Figure 6 while the red circles denote samples that were treated with a solution of DADPM after a pause time. On Figure 7, the red triangles show the data for the samples treated with a solution of AIBN. As pause time increases, the data show a clear decreasing trend in interfacial adhesion among all sample sets. This decreasing trend is due to the fact that when a layer is deposited, the heat rapidly dissipates from the surface of the newly deposited layer. This heat loss limits the intermolecular diffusion between the first layer and the next layer, decreasing inter-filament bonding.

The blue triangles on Figure 6 show that samples treated with the $CuSO_4$ solution did not demonstrate increased inter-filament bonding but rather a marked decrease below that of the neat ABS samples. This indicates that adding a Cu^{2+} suspension impedes rather than promotes interfacial adhesion. Although Cu^{2+} can form coordinating bonds with the nitrile, –CN, group at sufficiently high temperatures, the decrease in interfacial adhesion over both sets of samples suggests that coordinating

bonds were not formed in this work.

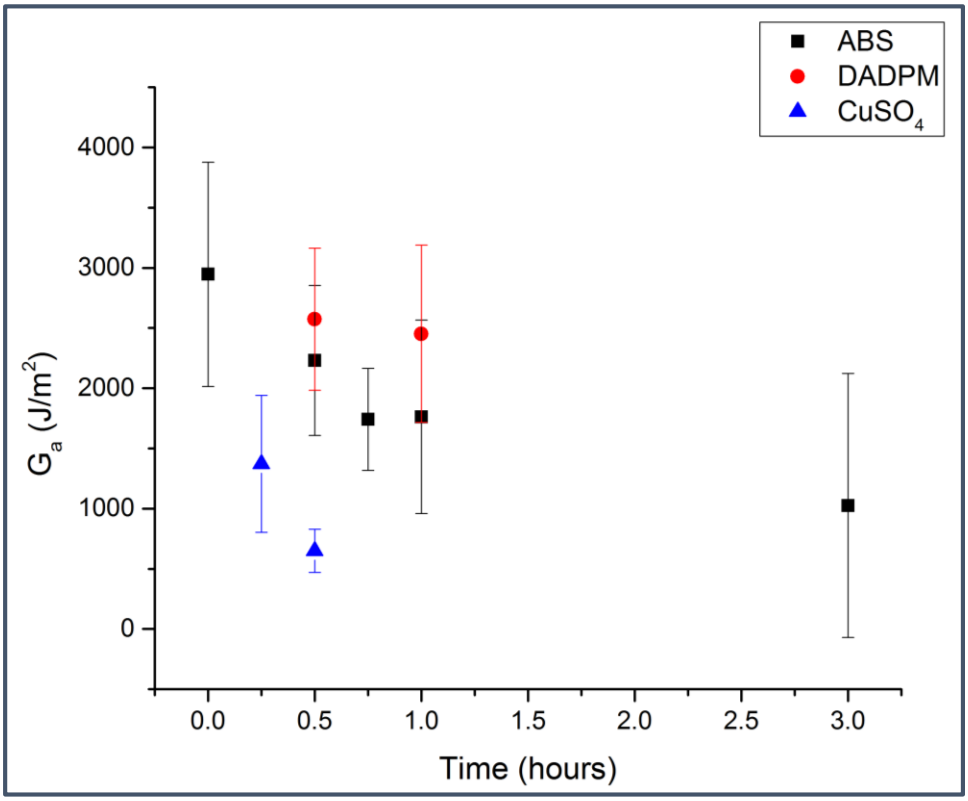

Figure 6: *Shows the interfacial adhesion data for the neat ABS, DADPM and $CuSO_4$-treated samples.*

One explanation for this phenomenon is that Cu^{2+} can also coordinate with water molecules, possibly acquired from the water vapor in the environment or from the acetone solution. The formation of strong coordination bonds with water prevents Cu^{2+} ions from coordinating to the nitrile groups on the deposited ABS filament. However, Cu^{2+} coordination to water molecules does not explain the marked decrease in inter-filament bond strength compared to the neat ABS samples. Restructuring on a molecular level could have occurred during the painting of the surface with the acetone solution reducing inter-filament bonding below that of the neat ABS, however, this phenomenon is not well-understood in the context of this research.

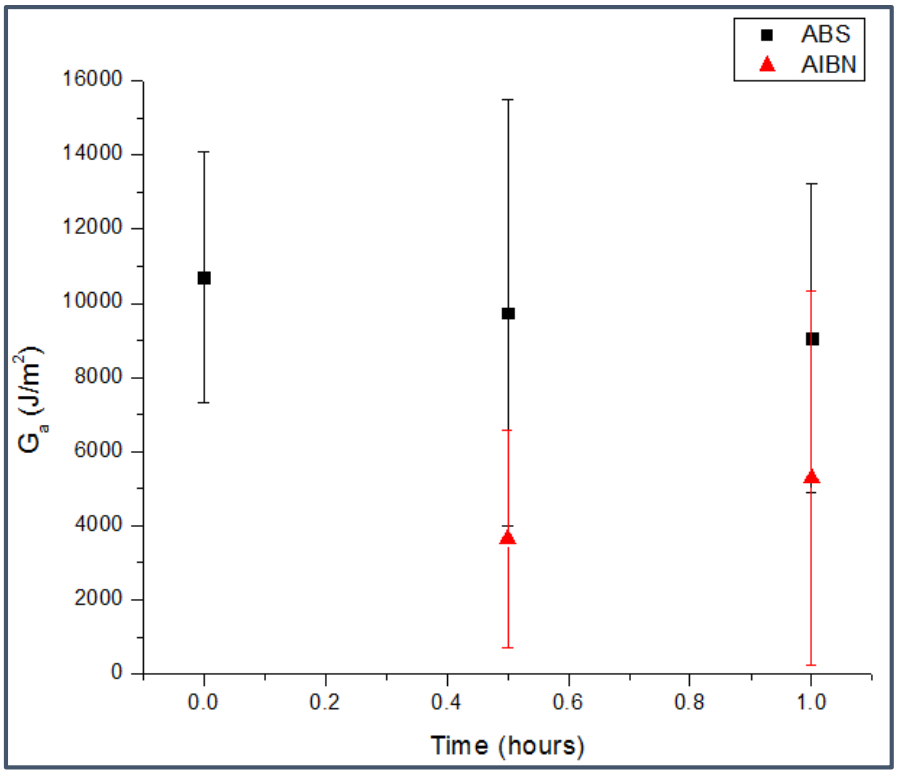

Figure 7: *Shows the Interfacial adhesion data for the neat ABS and AIBN treated samples.*

Figure 7 presents the surface adhesion data for neat ABS as well as ABS samples treated with AIBN initiator. The neat samples demonstrate the same downward trend in interfacial adhesion with increased pause times as discussed above. The figure also shows that the application of AIBN solution to the deposited layers resulted in a decrease in interfacial adhesion, indicating that the AIBN initiator solution, like the Cu^{2+} suspension, inhibits inter-filament bonding. A thermal initiator, AIBN decomposes above 65 ^{o}C to form two 2-cyanoprop-2-yl radicals. These radicals can initiate crosslinking between butadiene monomers within the ABS layers. The data suggest that this cross-linking did not occur since the interfacial adhesion decreased from that of neat ABS for samples with both 30 minute and 1 hour pause times. Even though the samples were printed at 210^{o}C with a bed temperature of 100^{o}C, the temperature of the top layer of

the bottom half of the printed t-peel part was found to be 52°C at a pause time of 0 minutes which suggests that the samples do not remain at temperatures high enough to decompose AIBN (Table 1).

Pause Time (minutes)	Temperature After Pause Time (°C)
0	52
30	46.8
60	33

Table 1: *Shows the temperature of the top layer of the bottom half of the t-peel part after pause times.*

Since the pause times for both sample sets were 30 or 60 minutes, the temperature of the samples had dropped well below 65 °C before the addition of AIBN. Also, as seen in the $CuSO_4$ samples, acetone evaporation could have further decreased the temperature of the layers. Both factors would result in a decrease in inter-filament bonding in AIBN-treated samples because the thermal environment of the layer is insufficient to react AIBN with the butadiene present.

When treated with DADPM solution, samples with pause times of 30 minutes and 1 hour displayed marked improvement in interfacial adhesion over that of neat ABS. This improvement indicates that DADPM chemically crosslinks the ABS layers, most likely through reactive functional groups. Pure ABS does not contain monomers with functional groups capable of reacting with DADPM. When exposed to heat and air, however, the polybutadiene (PB) segments of the ABS filament will undergo thermo-oxidative degradation to carboxyl groups. One study by Shimada and Kabuki demonstrated that the thermal oxidation of PB occurs at temperatures as low as 70-90 °C.[21] The process by which this occurs involves the formation of hydroperoxide radicals which collapse to hydroxyl and carboxyl groups. Since the samples in this experiment

were printed at 210 ^{o}C, the temperatures were sufficiently high to induce thermo-oxidative degradation of the PB monomers. If PB degradation occurs, the carboxyl groups can react with the terminal amine groups of DADPM to form covalent bonds between the deposited layers, probably via an amidization reaction.

Post-polymerization modification of ABS

The targeted structures for the cysteamine and DODT-modified ABS are shown in Figure 8.

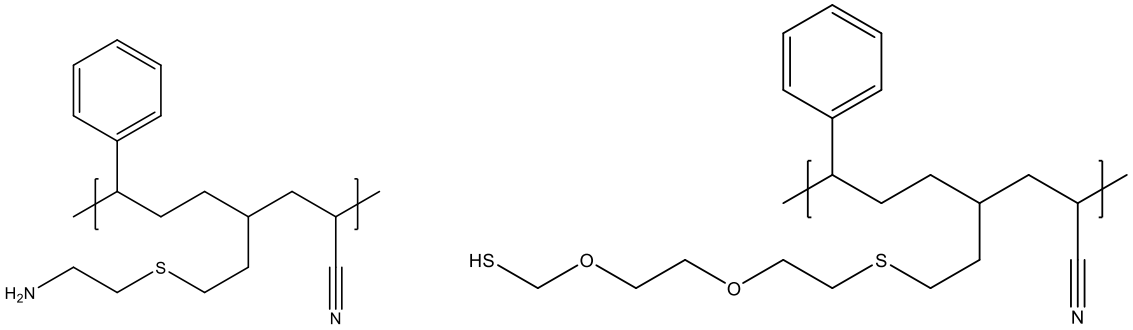

Figure 8: *Presents the targeted structures of cysteamine (L)-and DODT (R)-modified ABS in which the thiols have been added to the double bond of the butadiene within the polymer chain.*

^{1}H-NMR spectra obtained from the cysteamine and DODT-modified ABS are presented in Figures 8 and 9 and compared to that of neat ABS filament (Appendix). In the spectrum for the neat filament, the methyl region (0.9-2.0 ppm) contains a collection of peaks associated with proton resonances of the –CH_2 groups on the polymer chains. The broad peak corresponding to the proton resonances of the butadiene component occurs at 5.25 ppm. Further downfield between 6.5-7.5 ppm in the aromatic region, there is a cluster of peaks consistent with the deshielded protons of styrene.

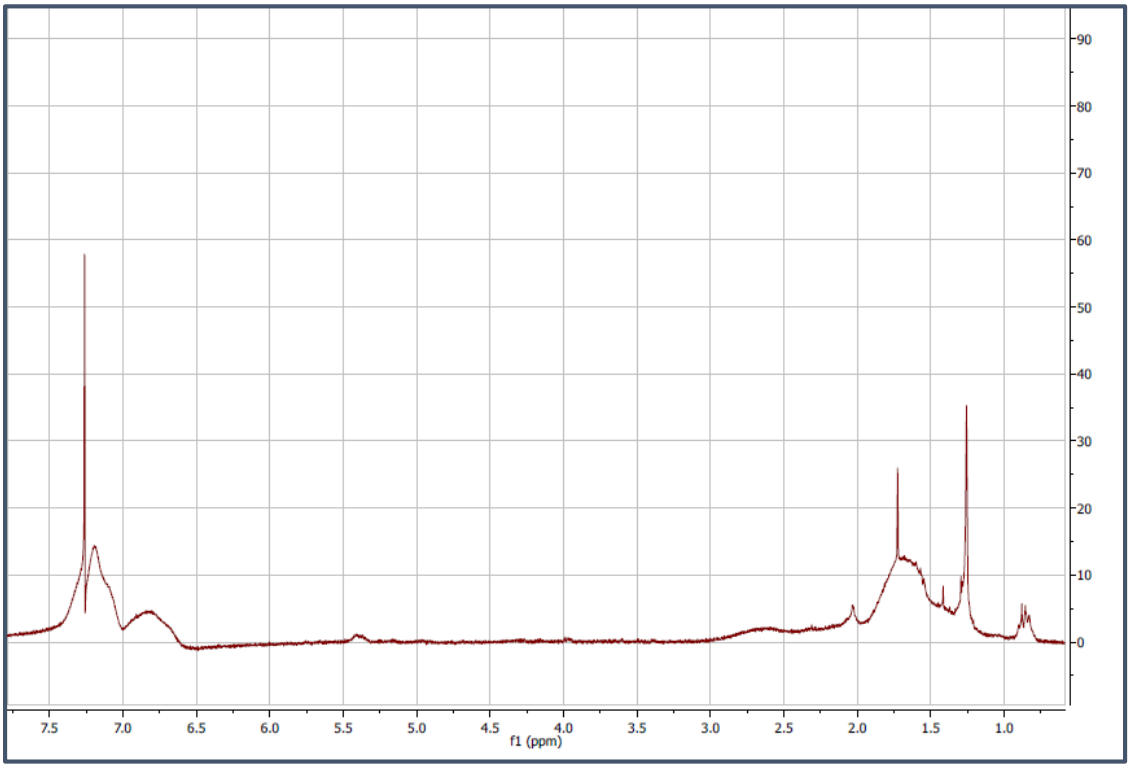

Figure 9: *Shows the ^{1}H-NMR spectrum of cysteamine-modified ABS.*

Figure 9 presents the spectrum obtained for cysteamine-modified ABS. A qualitative comparison of this spectrum with that of the non-modified ABS indicates that the three components are still present in the spectrum. Although the styrene peak remained unchanged as expected, the acrylonitrile and butadiene peaks, which occur in the regions of 2.0-2.5 ppm and 5.0-5.5 ppm respectively, show a marked decrease in size. This indicates that butadiene and acrylonitrile were lost in the reaction with cysteamine. The decrease in peak size suggests that butadiene underwent thiol modification. If modification occurred, a peak should also be visible consistent with the chemical shift of the protons of the cysteamine $–NH_2$ group. This is expected to occur in the 1.5-2.0 ppm region. From the spectrum, this region also corresponds to the resonances of the protons from the $–CH_2$ groups of the polymer chains. Therefore, the

presence of the thiol is indistinguishable in the cysteamine-ABS spectrum due to overlap with the $–CH_2$ groups.

The spectrum for the DODT-modified ABS is shown in Figure 10. Both the styrene and acrylonitrile peaks are still prominent but the butadiene peak is no longer present in the 5.0-5.5 ppm range. The lack of a butadiene peak suggests that butadiene reacted with DODT. To further reinforce the evidence for a reaction, there are peaks present at 2.75 ppm and 3.65 ppm that are consistent with the chemical shifts expected for the proton resonances of the DODT $–CH_2SH$ and $–OCH_2$ groups respectively. Qualitatively, the data suggest that the ABS was modified with DODT via the thiol-ene click reaction.

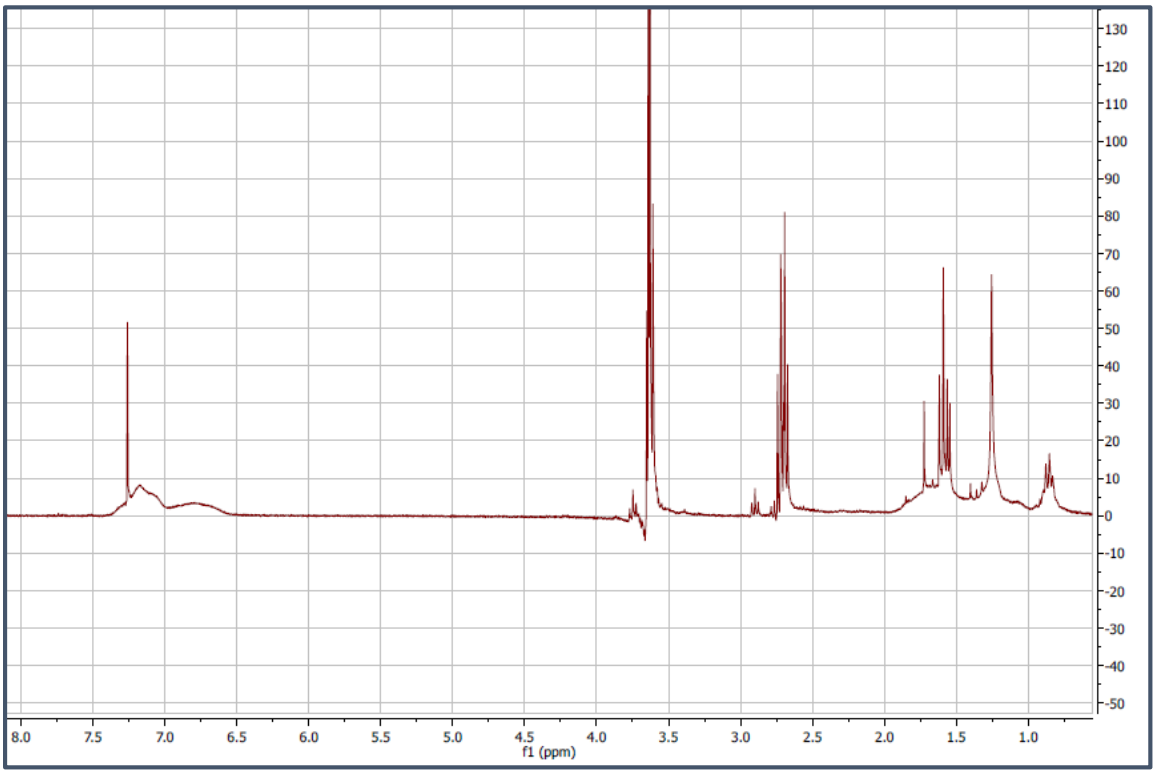

Figure 10: *Shows the ^{1}H-NMR spectrum for DODT-modified ABS.*

	% Acrylonitrile	% Butadiene	% Styrene	% Thiol
ABS Filament	25.1	12.2	62.7	0
Cysteamine-modified	indeterminate	1.17	62.7	indeterminate
DODT-modified	24.85	0	62.7	12.45

Table 2: *Presents a comparison of the percent composition of the cysteamine and DODT-modified ABS with non-modified ABS*

To quantify the amount of butadiene lost from the copolymer as well as the amount of thiol added, the percent compositions for each of the thiol-modified ABS were calculated from peak integration values and are presented in Table 2. For the ABS beads utilized in this experiment, acrylonitrile, styrene and butadiene comprise 25.1 %, 62.7 % and 12.2 % of the polymer chain respectively. If all of the butadiene reacted with the thiol, the percent butadiene composition would be 0% while the thiol would comprise 12.2 % of the ABS. Although the butadiene composition in the cysteamine-modified ABS decreased from 12.2 % to 1.17 %, quantitative calculations for the amount of thiol added were not possible due to the extensive peak overlap in the methyl region. In the DODT-modified ABS, however, the butadiene peak disappeared and the thiol peaks emerged at 2.75 ppm and 3.65 ppm, corresponding to a 12.45 % composition of the copolymer. This value is consistent with the expected thiol composition for the modified ABS if all of the butadiene was reacted and is a strong indicator that the thiol-ene “click” reaction allowed for effective post-polymerization modification of ABS.

Chapter 4: Conclusion

One of the major obstacles to utilizing FDM as an alternative to traditional manufacturing methods is the anisotropy affecting 3D printed parts. In this work, the application of a chemical cross-linker between deposited layers of ABS copolymer has been shown to reduce anisotropy by increasing inter-filament bonding in the z-direction. The mechanism for this cross-linking is not yet fully understood, however. Therefore, future studies should characterize the surface of the 3D printed layers to obtain an understanding of molecular orientation so that we can discover enhanced methods of chemical cross-linking that will result in improved mechanical properties.

Additionally, covalent modification of ABS was demonstrated through thiol post-polymerization methods. The disappearance of the butadiene peak in the ^{1}H-NMR spectra indicates that covalent bonds formed between the thiol and butadiene component of ABS through a thiol-ene “click” reaction. To further establish that the butadiene disappeared as a result of the thiol-ene reaction rather than reaction conditions, it would be necessary to perform the reaction utilizing ABS beads with no added thiol and then acquire the ^{1}H-NMR spectrum of the product. Butadiene lost through reaction conditions could then be accounted for in the thiol composition percentage. By demonstrating that ABS is capable of undergoing post-polymerization modification, pathways to utilize covalent bond formation between layers during the 3D printing process are provided, which could also lay a foundation for surface functionalization of the 3D printed parts. Building on these findings will allow us to design research to improve properties of 3D printed parts and transition from prototyping to mass manufacturing plastics using FDM technology.

References

1. Arivazhagan, A. & Masood, S. H. Dynamic Mechanical Properties of ABS Material Processed by Fused Deposition Modelling. *Int. J. Eng. Res. Appl.* **2,** 2009–2014 (2012).

2. Klein, P. W. *Fundamentals of plastics thermoforming*. (Morgan & Claypool Publishers, 2009).

3. Kroschwitz, J. I. *Concise encyclopedia of polymer science and engineering*. (Wiley, 1990).

4. Ozcelik, B., Ozbay, A. & Demirbas, E. Influence of injection parameters and mold materials on mechanical properties of ABS in plastic injection molding. *Int. Commun. Heat Mass Transf.* **37,** 1359–1365 (2010).

5. Bellini, A. & Guceri, S. Mechanical characterization of parts fabricated using fused deposition modeling. *Rapid Prototyp. J.* **9,** 252–264 (2003).

6. Caulfield, B., McHugh, P. E. & Lohfeld, S. Dependence of mechanical properties of polyamide components on build parameters in the SLS process. *J. Mater. Process. Technol.* **182,** 477–488 (2007).

7. Es-Said, O. S. *et al.* Materials and Manufacturing Processes Effect of Layer Orientation on Mechanical Properties of Rapid Prototyped Samples Effect of Layer Orientation on Mechanical Properties of Rapid Prototyped Samples. *Mater. Manuf. Process.* **15,** 107–122 (2000).

8. Ahn, S., Montero, M., Odell, D., Roundy, S. & Wright, P. K. Anisotropic material properties of fused deposition modeling ABS. *Rapid Prototyp. J.* **8,** 248–257 (2002).

9. Shofner, M. L., Lozano, K. & Rodrı, F. J. Nanofiber-Reinforced Polymers Prepared by Fused Deposition Modeling. (2002).

10. Zhong, W., Li, F., Zhang, Z., Song, L. & Li, Z. Short fiber reinforced composites for fused deposition modeling. *Mater. Sci. Eng. A* **301,** 125–130 (2001).

11. Ibarra, L. & Alzorriz, M. Ionic elastomers based on carboxylated nitrile rubber and magnesium oxide. *J. Appl. Polym. Sci.* **103,** 1894–1899 (2007).

12. Kashif, M. & Chang, Y. W. Preparation of supramolecular thermally repairable elastomer by crosslinking of maleated polyethylene-octene elastomer with 3-amino-1,2,4-triazole. *Polym. Int.* **63,** 1936–1943 (2014).

13. Iijima, T., Yoshioka, N. & Tomoi, M. Effect of cross-link density on modification of epoxy resins with reactive acrylic elastomers. *Eur. Polym. J.* **28,** 573–581 (1992).

14. Shaffer, S., Yang, K., Vargas, J., Di Prima, M. A. & Voit, W. On reducing anisotropy in 3D printed polymers via ionizing radiation. *Polymer (Guildf).* **55,** 5969–5979 (2014).

15. Gauthier, M. A., Gibson, M. I. & Klok, H.-A. Synthesis of Functional Polymers by Post-Polymerization Modification. *Angew. Chemie Int. Ed.* **48,** 48–58 (2009).

16. Justynska, J. & Schlaad, H. Modular synthesis of functional block copolymers. *Macromol. Rapid Commun.* **25,** 1478–1481 (2004).

17. Fairbanks, B. D. *et al.* A Versatile Synthetic Extracellular Matrix Mimic via Thiol-Norbornene Photopolymerization. *Adv. Mater.* **21,** 5005–5010 (2009).

18. Cramer, N. B. *et al.* Investigation of thiol-ene and thiol-ene–methacrylate based resins as dental restorative materials. *Dent. Mater.* **26,** 21–28 (2010).

19. Yang, H. *et al.* Thermo-sensitive electrospun fibers prepared by a sequential thiol-ene click chemistry approach. *J. Polym. Sci. Part A Polym. Chem.* **50,** 4182–4190 (2012).

20. Campos, L. M. *et al.* Development of Thermal and Photochemical Strategies for Thiol−Ene Click Polymer Functionalization. *Macromolecules* **41,** 7063–7070 (2008).

21. Shimada, J. & Kabuki, K. The mechanism of oxidative degradation of ABS resin. Part II. The mechanism of photooxidative degradation. *J. Appl. Polym. Sci.* **12,** 671–682 (1968).

Appendix

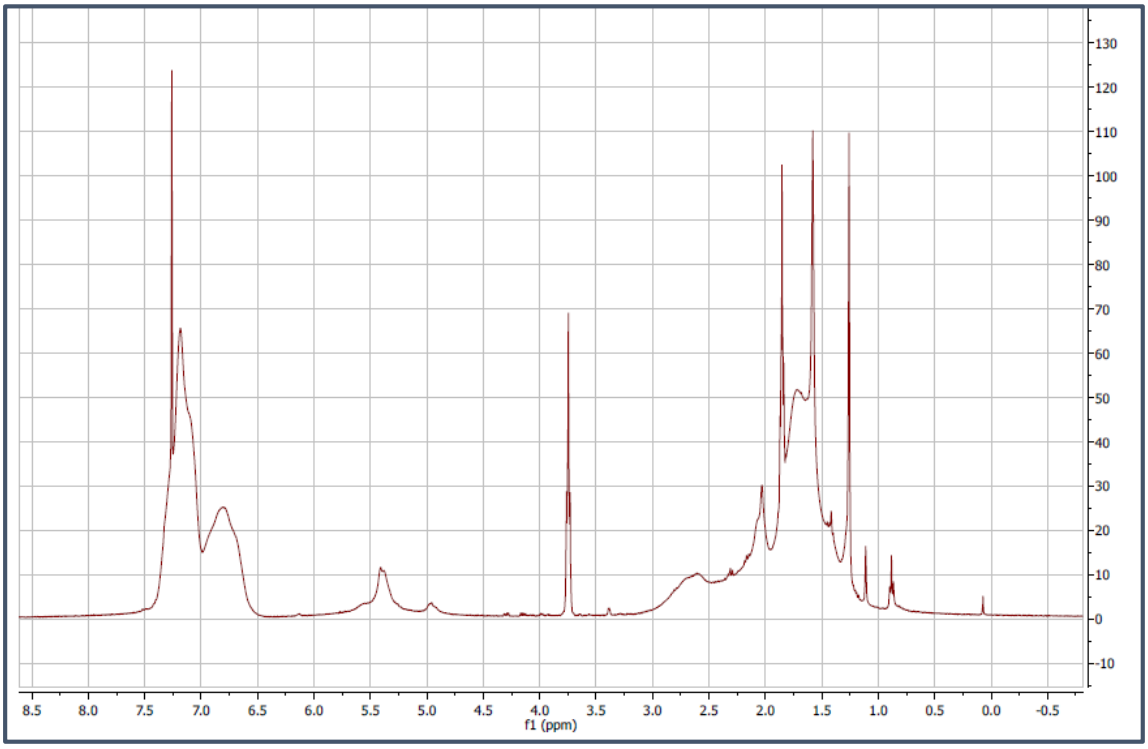

Shows the ^{1}H-NMR spectrum for non-modified ABS.